Bioorganic & Medicinal Chemistry Letters 21 (2011) 1607–1611

Contents lists available at ScienceDirect

Bioorganic & Medicinal Chemistry Letters

journal homepage: www.elsevier.com/locate/bmcl

Computational study of bindings of HL9, a nonapeptide fragment of human lysozyme, to HIV-1 fusion protein gp41

Yossa Dwi Hartono [a], Angelina Noviani Lee [a], Sylvia Lee-Huang [b], Dawei Zhang [a,*]

[a] Division of Chemistry and Biological Chemistry, School of Physical and Mathematical Sciences, Nanyang Technological University, Singapore 637371, Singapore
[b] Department of Biochemistry, New York University Langone Medical Center, New York, NY 10016, USA

ARTICLE INFO

Article history:
Received 14 September 2010
Revised 19 January 2011
Accepted 26 January 2011
Available online 2 February 2011

Keywords:
HIV-1 gp41
Human lysozyme
HL9

ABSTRACT

HL9 is a nonapeptide fragment of human lysozyme which has been shown to have anti-HIV-1 activity in nanomolar concentration. This study aims to explain this inhibitory activity by using molecular dynamics (MD) simulation, focusing on the ectodomain of gp41, the envelope glycoprotein of HIV-1 crucial to membrane fusion. It was found that in HL9, two Trp residues separated by two others occupy the conserved hydrophobic pocket on gp41 and thus inhibit fusion in dominant-negative manner. Detailed HL9-gp41 binding interactions and free energies of binding were obtained through MD simulation and solvated interaction energies (SIE) calculation, giving a binding free energy of −8.25 kcal/mol which is in close agreement with the experimental value of −9.96 kcal/mol. Since C-helical region (C34) of gp41 also has two Trp residues separated by two others, this arrangement may be generalised and used to scan peptide library and to find those having similar manner of inhibition.

The entry of HIV-1 is facilitated by the envelope glycoproteins (Env), comprising trimers of gp120 and those of gp41. When gp120 binds to its major cellular receptor, CD4, and possibly other co-receptors, it undergoes conformational change such that gp41 ectodomain is exposed. This ectodomain contains the crucial fusion machinery: fusion peptide that attaches to the target cell membrane, trimeric N-heptad repeats (NHR/N36), and trimeric C-heptad repeats (CHR/C34); each pair of monomers of the latter two are connected by a 30-residue loop.[1] The crystal structure omits the fusion peptide, the connecting loops and the glycosyl moieties,[2] leaving a trimer-of-hairpins configuration in which N36 forms the central trimeric coiled-coil being flanked by C34 in oblique and anti-parallel manner.[3] This post-fusion state is also called six-helix bundle (6-HB). The free energy released by formation of this stable configuration drives membrane fusion.[4]

Synthetic C-peptides have been shown to inhibit fusion in nanomolar concentration. Specifically, it binds to the prehairpin intermediate at the N-peptide region downstream the fusion peptide, thereby inhibiting in a dominant-negative manner.[5] This N-peptide region has a hydrophobic pocket containing residues Leu-565′, Leu-566, Leu-568, Thr-569, Thr-569′, Val-570, Trp-571′, Gly-572′, Ile-573, Ile-573′, Lys-574, Leu-576 and Gln-577 (A *prime* (′) indicates residue belonging to the adjacent N-peptide monomer); receiving side chains of Ile-635, Asp-632, Trp-631 and Trp-628 on the C-peptide.[2]

Previously, it was human chorionic gonadotropin (hCG) β-core preparation that was discovered to have anti-HIV-1 activity, causing low rate of vertical HIV-1 transmission during first trimester of gestation.[6,7] Upon fractionation, it was found that a protein with sequence identical to human lysozyme exhibits activity comparable to the authentic lysozyme.[8] Further antiviral assays of several kinds of lysozymes then reveal that they all have anti-HIV-1 activity.[8] Peptide fragmentation and activity mapping of human lysozyme were then carried out. The smallest fragment retaining the anti-HIV-1 activity of human lysozyme was found to be a nonapeptide, dubbed HL9 (Fig. 1a). The antiviral activity was measured by microtiter syncytium formation and p24 expression assays.[9] Compared with enfuvirtide (a 36-residue peptide approved by FDA in 2003), the only available HIV-1 entry inhibitor in the market, HL9 is attractive as fusion inhibitor due to its short length and low cost to synthesise.[10] However, HL9 still also shares the same weaknesses as enfuvirtide: lack of oral bioavailability and short in vivo half-life due to blood proteolytic enzymes.[10] Therefore, modifications such as cross-linking and substitution with unnatural helix-favouring amino acids may be applied to HL9 to confer better oral bioavailability and longer in vivo half-life. Such modifications have been done on other short peptides to improve binding strength.[11] In this work, our study aims to complement the experimental data by performing computational simulation as to elucidate the inhibitory mechanism of HL9. Molecular dynamics (MD) simulation is performed to investigate molecular interactions, stability of the binding complex, and binding affinities of HL9 to gp41.

In this work, HIV-1 gp41 crystal structure was obtained from Protein Data Bank (PDB ID: 1AIK).[2] HL9 construction was carried

* Corresponding author.
E-mail address: zhangdw@ntu.edu.sg (D. Zhang).

0960-894X/$ - see front matter © 2011 Elsevier Ltd. All rights reserved.
doi:10.1016/j.bmcl.2011.01.121

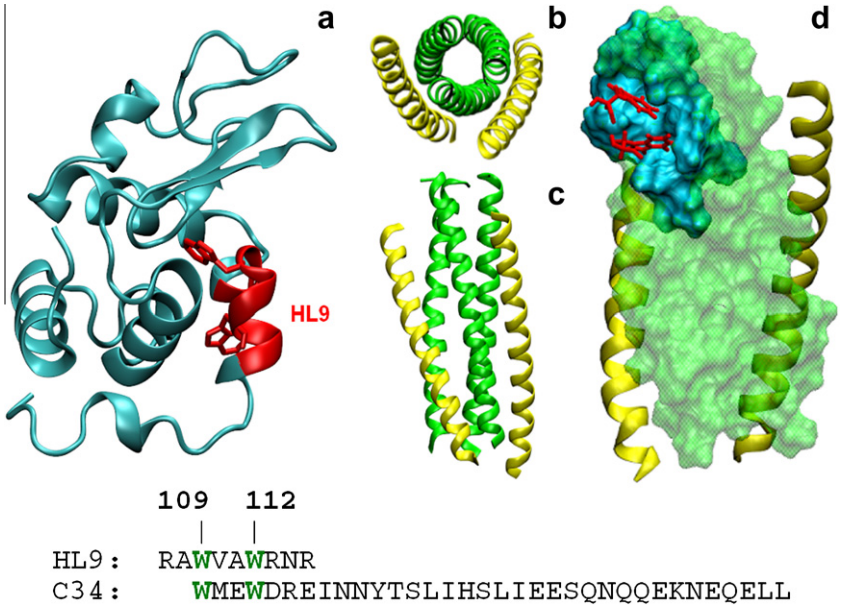

Figure 1. (a) HL9 (red) in human lysozyme (cyan); 5-HB consisting of two C34 (yellow) and three N36 (green) helices: (b) top view, (c) side view showing oblique and anti-parallel flanking of C34 and (d) hydrophobic binding pocket (blue) formed by two N36 helices, occupied by two Trp sidechains (red); Both HL9 and C34 sequences are also shown for comparison.

out using LEaP module, while molecular dynamics simulations were carried out using SANDER module; both modules are of AMBER 9.0 program[12] with ff03 force field.[13] TIP3P water molecules were added with the minimal distance between the complex and the edge of water box set as 10 Å. Three K^+ counterions were added to maintain neutrality of the system. Non-bonded cutoff was set to 12.0 Å. SHAKE algorithm[14] was applied with all bonds involving hydrogen atoms restrained. After minimisation and heating up from 10 to 300 K for 100 ps, productive MD was carried out at 300 K, with timestep of 2.0 fs for 3000 ps period, with complex conformations collected every 1 ps.

For post-processing analysis and binding free energy calculation, all water molecules, counterions and periodic boundary information were removed from the trajectory. Single-trajectory approach was used for all binding free energy calculations.[15–17] 500 regular snapshots from time interval with stable fluctuation (one snapshot every 5 ps between 0.5 and 3.0 ns) were used for MM-PBSA of AMBER 9.0 and solvated interaction energy (SIE) using sietraj[18,19] to calculate binding free energy. Electrostatic contribution to desolvation was calculated with numerical solver of Poisson-Boltzmann method, as implemented in PBSA programme.[20] Non-polar contribution to desolvation was determined with solvent-accessible-surface-area-dependent term. Surface area was determined using analytical ideas of Connolly,[21] as implemented in MOLSURF programme. One hundred regular snapshots from the same time interval (one snapshot every 50 ps between 0.5 and 3.0 ns) were used for normal mode analysis (Nmode) to complement MM-PBSA data with entropy contribution. RMSD and hydrogen bonding analyses were carried out using ptraj module of AMBER 9.0. For hydrogen bonding, distance and angle cutoffs are 3.0 Å and 120°, respectively. All simulation images were generated using VMD.[22]

In this study, one C34 was removed from the six-helix bundle to expose the hydrophobic binding pocket formed by two N36 so as to simulate the prehairpin intermediate. Henceforth this receptor protein is referred to as 5-HB (Fig. 1b). We hypothesised that HL9 binds the aforementioned hydrophobic binding pocket at N-peptide. There are several reasons to formulate such a specific hypothesis: First, HL9 prevents syncytia formation, which is indicative of membrane fusion, and p24 expression, which is indicative of viral replication. Thus, inhibition has to occur upstream in the viral infectivity pathway, before viral entry. The obvious target is thus Env, which facilitates viral entry. HIV-1 gp120 has interspersed variable loops, whereas gp41 has more conserved sequence, especially at the hydrophobic pocket.[2,23] Thus, gp41 is a more likely target of a fusion inhibitor. Second, HL9 shares sequence similarity with the C-peptide. It has two Trp residues separated by two other residues (Fig. 1). As mentioned, Trp-628 and Trp-631 of C-peptide are important side chains binding to the conserved hydrophobic cavity of N-peptide. The two Trp residues and how far they are apart are crucial to HL9 inhibitory activity. Scrambled (AWRWRARVN) and W-to-Y mutated (RAYVAWKNR, RAWVAYRNR) HL9 have no activity in both assays.[9]

Since peptide–peptide docking is computationally demanding, docking in this study was carried out in a simple and manual way. Our hypothesis is that HL9 would inhibit in dominant-negative manner. The two Trp residues are of special interest, as explained above. We conjectured that the main interaction in inhibition process would involve the two Trp sidechains. So we poised the two Trp sidechains towards the binding pocket, then the other residues were added. Since there are two Trp residues and two Trp sites, there are two possibilities in which the Trp residues of HL9 can occupy those sites. MD simulations were therefore performed for two binding modes of HL9 (Fig. 2). In one mode, MD1, Trp-109 occupies the groove nearer to the carboxy-terminal while Trp-112 occupies the distal groove. In the other mode, MD2, Trp-112 occupies the nearer groove; Trp-109, the distal groove. In both modes, HL9 is approximately oblique with respect to the trimeric N36 core, similar to C34 binding orientation.[3] The system was well equilibrated after 500 ps and for the rest of the MD simulations, RMSD fluctuations for both 5-HB and HL9 for both modes are within reasonably narrow range.

For both modes, trajectory snapshots were collected for molecular mechanics Poisson-Boltzmann surface area (MM-PBSA)/solvated interaction energy (SIE) calculation and normal mode analysis. Normal mode analysis was done over fewer snapshots since it is more computationally expensive.[23] Binding free energies and their energy term breakdowns as average over the snapshots

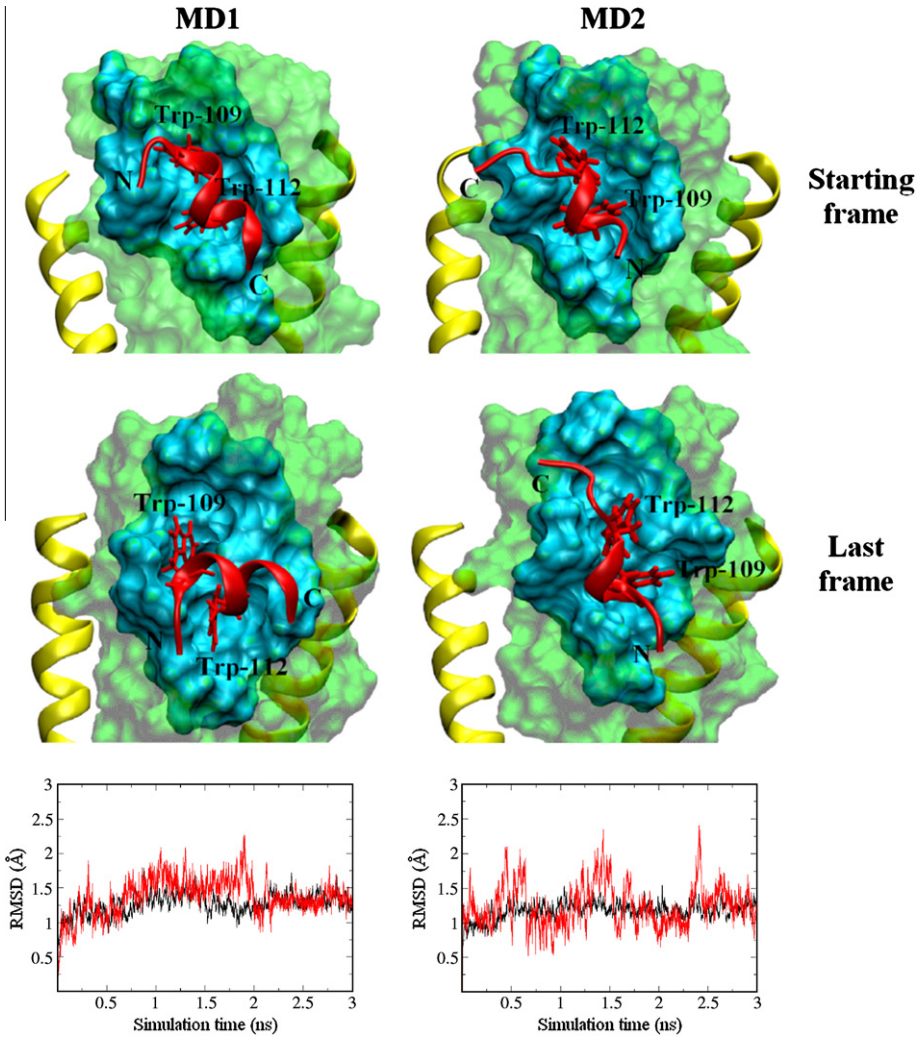

Figure 2. Top: two binding modes of HL9 (first frame), middle: last frames of MD simulations and bottom: root-mean-square deviations (RMSD) of 5-HB (black) and HL9 (red) during MD simulations.

are presented in Table 1. Also shown are the experimental EC_{50} values[9] which have been converted to binding free energies. SIE and MM-PBSA–Nmode predict similar value of binding free energy for MD2, with difference of 1.53 kcal/mol, whereas for MD1 SIE and MM-PBSA–Nmode disagree significantly by 13.79 kcal/mol. However, both methods agree that MD2 is the more favourable binding mode. SIE predicts value nearer to the experimental value. The more accurate prediction by SIE calculation is not surprising. The underlying principles used in MM-PBSA and SIE are similar, but SIE is further empirically calibrated using diverse datasets of absolute binding free energies from 99 protein–ligand complexes.[18]

The last frames of the simulation (Fig. 2) reveal that in MD1, HL9 is approximately perpendicular with respect to the trimeric N36 core, while in MD2, HL9 is oblique. The latter orientation is evidently more favourable for binding. This arrangement is similar to how C34 binds to N36 in trimer-of-hairpins. Fig. 3a depicts HL9 as superimposed to C34 using backbone fitting (HL9: Trp-109 to Trp-112, C34: Trp-628 to Trp-631). The RMSD for this fitting is 0.6 Å. Since MD2 yields a more favourable binding free energy compared to MD1, further analyses are focussed on MD2.

Computational alanine-scanning mutagenesis was carried out to determine the contribution of each residue of HL9 to binding free energy. The final value of MM-PBSA, $\Delta G_{\text{MM-PBSA}}$, comprises polar ($\Delta E_{\text{ele}} + \Delta G_{\text{PB}}$) and non-polar contributions ($\Delta E_{\text{VDW}} + \Delta G_{\text{SA}}$):

$$\Delta G_{\text{MM-PBSA}} = (\Delta E_{\text{ele}} + \Delta G_{\text{PB}}) + (\Delta E_{\text{VDW}} + \Delta G_{\text{SA}}) \quad (1)$$

The energy terms for each mutant are then normalised the energy terms of wild-type HL9 (Fig. 4). This was done by expressing the energy terms of each mutant as fractions of the corresponding energy terms of wild-type HL9. Observed decrease in normalised energy terms indicates that the residue in consideration contributes to binding, since mutating it to Ala reduces $\Delta G_{\text{MM-PBSA}}$ value. Based on Fig. 4, residues which are important to binding are Trp-109 and Trp-112. The two Trp residues contribute significantly to both polar and non-polar terms.

The two Trp residues contribute equally. This is also supported by the RMSD data of the two Trp sidechains (Fig. 3c). The stability of the two sidechains is similar, indicating that their binding interactions are equally favourable. When both Trp are mutated to Ala, $\Delta G_{\text{MM-PBSA}}$ of this mutant is only 42% that of the wild-type, therefore overall contribution of both Trp residues is approximately 58%. Other residues do not exhibit significant contributions, except for the terminal Arg residues which exhibit slight contributions, presumably due to their charged nature.

Only hydrogen bonding between 5-HB and HL9 are considered. Two residues of HL9, Trp-109 and Asn-114, are involved in hydrogen bonding (Fig. 3b). The hydrogen bond between acceptor carbonyl oxygen of Leu-568 (5-HB) and donor N-hydrogen of the indole ring of Trp-109 (HL9) has 78.8% occupancy. The other four

Table 1
Average binding free energies for HL9 and 5-HB, standard error in parentheses (all values in kcal/mol)

MD1					
MM-PBSA			SIE		
ΔE_{ele}	−181.50	(1.55)	E_C	−80.70	(0.69)
ΔE_{VDW}	−38.30	(0.22)	E_{VDW}	−38.30	(0.22)
ΔG_{PB}	201.86	(1.47)	ΔG^R_{bind}	89.22	(0.62)
ΔG_{SA}	−5.81	(0.02)	$\gamma\Delta$MSA	−7.36	(0.04)
$\Delta G_{MM\text{-}PBSA}$	−23.76	(0.31)	K	−2.89	(0.00)
Nmode					
$T\Delta S$	−30.77	(0.47)			
ΔG	+7.01	(0.56)	ΔG	−6.78	(0.03)
MD2					
MM-PBSA			SIE		
ΔE_{ele}	−167.77	(1.00)	E_C	−74.59	(0.45)
ΔE_{VDW}	−48.67	(0.18)	E_{VDW}	−48.67	(0.18)
ΔG_{PB}	187.23	(0.90)	ΔG^R_{bind}	81.63	(0.40)
ΔG_{SA}	−7.20	(0.02)	$\gamma\Delta$MSA	−9.56	(0.03)
$\Delta G_{MM\text{-}PBSA}$	−36.41	(0.23)	K	−2.89	(0.00)
Nmode					
$T\Delta S$	−29.69	(0.53)			
ΔG	−6.72	(0.58)	ΔG	−8.25	(0.02)

ΔG (microtiter syncytia formation assay) = −10.02.
ΔG (p24 expression assay) = −9.96.

hydrogen bonds involving Asn-114 are more transient, ranging from 1.3% to 7.7% occupancies. The hydrogen bonds are not likely to be the major interactions contributing to the polar terms. Alanine-scanning (Fig. 4) shows that Trp-109 and Trp-112 have approximately equal polar contributions, while only Trp-109 has hydrogen bond among the two Trp residues. Also, if this hydrogen bond is the major interaction, RMSD between the two Trp sidechains would have differed much; Trp-109 would appear more stable with the hydrogen bond anchor. However, this is not the case (Fig. 3c). The polar contributions of Trp-109 and Trp-112 then must have come from other polar interactions, such as permanent dipole–permanent dipole interaction and charged–permanent dipole interaction.

In summary, binding of HL9 to HIV-1 gp41 5-helix bundle was simulated from MD calculations. Binding free energy was analysed using MM-PBSA, normal mode analysis, and SIE. The simulation showed that the highly-conserved hydrophobic cavity formed by two N36 helices is the most possible binding site. It is occupied by C34 in the post-fusion conformation of gp41, but is exposed in the prehairpin intermediate. Thus, HL9 may compete with C34 for the same binding site, inhibiting in dominant-negative manner, preventing the formation of six-helix bundle, whose free energy of formation is necessary to drive membrane fusion.[4]

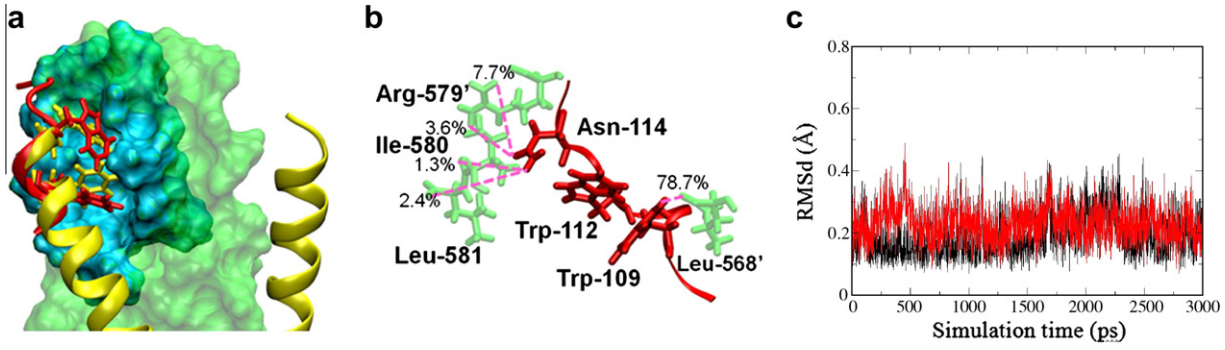

Figure 3. (a) HL9 in MD2 superimposed with C34, (b) hydrogen bonding of HL9 in MD2 with % occupancies and (c) sidechain RMSD of Trp-109 (black) and Trp-112 (red).

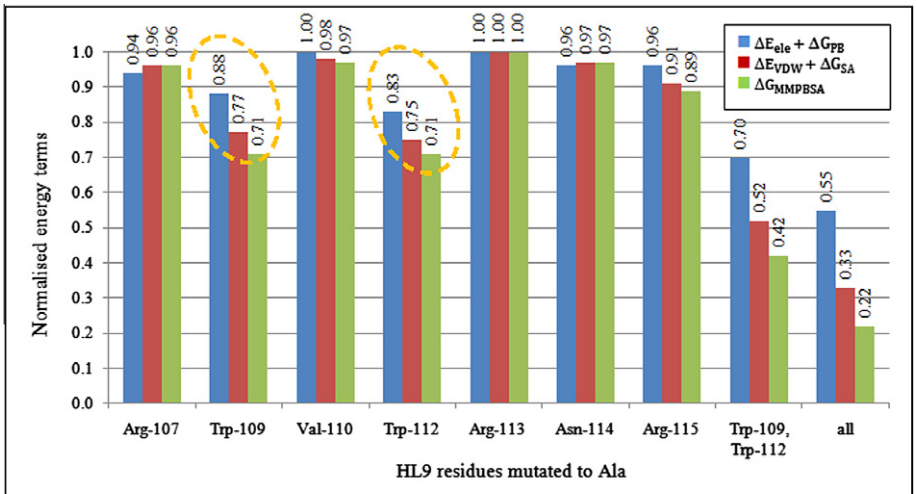

	Arg-107	Trp-109	Val-110	Trp-112	Arg-113	Asn-114	Arg-115	Trp-109, Trp112	all	Wild-type HL9
$\Delta E_{ele} + \Delta G_{PB}$	18.28	17.2	19.55	16.15	19.38	18.69	18.67	13.62	10.69	**19.46**
$\Delta E_{VDW} + \Delta G_{SA}$	-53.36	-43.03	-54.81	-42.06	-55.64	-54.1	-51.09	-28.95	-18.57	**-55.87**
ΔG_{MMPBSA}	-35.08	-25.83	-35.26	-25.91	-36.26	-35.41	-32.42	-15.33	-7.88	**-36.41**

Figure 4. Single-structure based computational alanine-scanning of HL9. Absolute values shown in kcal/mol.

Previous study identified small molecule inhibitors—oleuropein and hydroxytyrosol—which target the same hydrophobic binding pocket and inhibit viral fusion in nanomolar concentrations.[24] Despite the similarities, the interactions are different. For example, for the small molecule inhibitors, hydrogen bonding with Gln-577/Gln-575 is important, while in MD2 no such hydrogen bond is present.[24] Hydrophobic interactions may prove to be more similar, though this will require further analysis of the trajectories from the previous and current studies. Dissimilarities notwithstanding, details of binding interactions from these inhibitors may provide important clues to design a more potent inhibitor.

It is also important to note that the most important interactions come from the two Trp residues which are separated by two other residues. These two interspersed residues do not seem to affect binding to 5-HB since the sidechains point to the opposite those of Trp residues. Future research thus may be directed to peptides having two Trp residues separated by two others. Further modifications should be focussed on stabilising the Trp sidechains and less so on modifications designed to improve overall helical propensity.

Acknowledgements

D.W.Z. is supported in part by Nanyang Technological University start-up Grant, and in part by Singapore AcRF Tier 1 Grant of M52110095.

References and notes

1. Frey, G.; Rits-Volloch, S.; Zhang, X.-Q.; Schooley, R. T.; Chen, B.; Harrison, S. C. *Proc. Natl. Acad. Sci. U.S.A.* **2006**, *103*, 13938.
2. Chan, D. C.; Fass, D.; Berger, J. M.; Kim, P. S. *Cell* **1997**, *89*, 263.
3. Eckert, D. M.; Kim, P. S. *Annu. Rev. Biochem.* **2001**, 777.
4. Melikyan, G. B.; Markosyan, R. M.; Hemmati, H.; Delmedico, M. K.; Lambert, D. M.; Cohen, F. S. *J. Cell Biol.* **2000**, *151*, 413.
5. Lu, M.; Blacklow, S.; Kim, P. S. *Nat. Struct. Mol. Biol.* **1995**, *2*, 1075.
6. Rossi, A. D.; Ometto, L.; Mammano, F.; Zanotto, C.; Giaquinto, C.; Chieco-Bianchi, L. *AIDS* **1992**, *6*, 1117.
7. Krivine, A.; Cao, L.; Lebon, P.; Francoual, C.; Firtion, G.; Henrion, R. *Lancet* **1992**, *339*, 1187.
8. Lee-Huang, S.; Huang, P. L.; Sun, Y.; Kung, H. F.; Blithe, D. L.; Chen, H. C. *Proc. Natl. Acad. Sci. U.S.A.* **1999**, *96*, 2678.
9. Lee-Huang, S.; Maiorov, V.; Huang, P. L.; Ng, A.; Lee, H. C.; Chang, Y.-T.; Kallenbach, N.; Huang, P. L.; Chen, H.-C. *Biochemistry* **2005**, *44*, 4648.
10. Liu, S.; Wu, S.; Jiang, S. *Curr. Pharm. Des.* **2007**, *13*, 143.
11. Sia, S. K.; Carr, P. A.; Cochran, A. G.; Malashkevich, V. N.; Kim, P. S. *Proc. Natl. Acad. Sci. U.S.A.* **2002**, *99*, 14664.
12. D.A. Case, T.A. Darden, T.E. Cheatham, III, C.L. Simmerling, J. Wang, R.E. Duke, R., Luo, K.M. Merz, D.A. Pearlman, M. Crowley, R.C. Walker, W. Zhang, B. Wang, S., Hayik, A. Roitberg, G. Seabra, K.F. Wong, F. Paesani, X. Wu, S. Brozell, V. Tsui, H., Gohlke, L. Yang, C. Tan, J. Mongan, V. Hornak, G. Cui, P. Beroza, D.H. Mathews, C., and Schafmeister, W.S. Ross, A. P. A. K. **2006**; AMBER 9, University of California, San Francisco.
13. Duan, Y.; Wu, C.; Chowdhury, S.; Lee, M. C.; Xiong, G.; Zhang, W.; Yang, R.; Cieplak, P.; Luo, R.; Lee, T.; Caldwell, J.; Wang, J.; Kollman, P. *J. Comput. Chem.* **2003**, *24*, 1999.
14. Ryckaert, J.; Ciccotti, G.; Berendsen, H. *J. Comp. Phys.* **1977**, *23*, 327.
15. Srinivason, J.; Cheatham, T. E., III; Cieplak, P.; Kollman, P. A.; Case, D. A. *J. Am. Chem. Soc.* **1998**, *120*, 9401.
16. Kollman, P. A.; Massova, I.; Reyes, C.; Kuhn, B.; Huo, S.; Chong, L.; Lee, M.; Lee, T.; Duan, Y.; Wang, W.; Donini, O.; Cieplak, P.; Srinivason, J.; Case, D. A.; Cheatham, T. E., III *Acc. Chem. Res.* **2000**, *33*, 889.
17. Tsui, V.; Case, D. A. *J. Phys. Chem. B* **2001**, *105*, 11314.
18. Naïm, M.; Bhat, S.; Rankin, K. N.; Dennis, S.; Chowdhury, S. F.; Siddiqi, I.; Drabik, P.; Sulea, T.; Bayly, C. I.; Jakalian, A.; Purisima, E. O. *J. Chem. Inf. Model.* **2007**, *47*, 122.
19. Cui, Q.; Sulea, T.; Schrag, J. D.; Munger, C.; Hung, M.-N.; Naïm, M.; Cygler, M.; Purisima, E. O. *J. Mol. Biol.* **2008**, *379*, 787.
20. Luo, R.; David, L.; Gilson, M. K. *J. Comput. Chem.* **2002**, *23*, 1244.
21. Connolly, M. L. *J. Appl. Crystallogr.* **1983**, *16*, 548.
22. Humphrey, W.; Dalke, A.; Schulten, K. *J. Mol. Graph.* **1996**, *14*, 33. 27–28.
23. Bao, J.; Zhang, D. W.; Zhang, J. Z. H.; Huang, P. L.; Huang, P. L.; Lee-Huang, S. *FEBS Lett.* **2007**, *581*, 2737.
24. Lee-Huang, S.; Huang, P. L.; Zhang, D.; Lee, J. W.; Bao, J.; Sun, Y.; Chang, Y.-T.; Zhang, J.; Huang, P. L. *Biochem. Biophys. Res. Commun.* **2007**, *354*, 872.